Geophysical Research Letters

RESEARCH LETTER
10.1029/2019GL082692

The Equatorial Undercurrent and the Oxygen Minimum Zone in the Pacific

Julius J. M. Busecke[1], Laure Resplandy[1], and John P. Dunne[2]

Department of Geosciences,[1] Princeton University, Princeton, NJ, USA, [2]NOAA Geophysical Fluid Dynamics Laboratory, Princeton, NJ, USA

Key Points:
- The Equatorial Undercurrent dynamics control the structure of the oxygen minimum zone (OMZ) in the equatorial Pacific
- The mean shape of the OMZ subsequently influences its temporal variability
- Models with unrealistic OMZ shape are too sensitive to changes in circulation, impeding their ability to project future OMZ changes

Supporting Information:
- Supporting Information S1

Correspondence to:
J. J. M. Busecke,
jbusecke@princeton.edu

Citation:
Busecke, J. J. M., Resplandy, L., & Dunne, J. P. P. (2019). The Equatorial Undercurrent and the oxygen minimum zone in the Pacific. *Geophysical Research Letters*, *46*, 6716–6725. https://doi.org/10.1029/2019GL082692

Received 5 MAR 2019
Accepted 14 MAY 2019
Accepted article online 20 MAY 2019
Published online 19 JUN 2019
Corrected 26 AUG 2019

This article was corrected on 26 AUG 2019. See the end of the full text for details.

Abstract Warming-driven expansion of the oxygen minimum zone (OMZ) in the equatorial Pacific would bring very low oxygen waters closer to the ocean surface and possibly impact global carbon/nutrient cycles and local ecosystems. Global coarse Earth System Models (ESMs) show, however, disparate trends that poorly constrain these future changes in the upper OMZ. Using an ESM with a high-resolution ocean (1/10°), we show that a realistic representation of the Equatorial Undercurrent (EUC) dynamics is crucial to represent the upper OMZ structure and its temporal variability. We demonstrate that coarser ESMs commonly misrepresent the EUC, leading to an unrealistic "tilt" of the OMZ (e.g., shallowing toward the east) and an exaggerated sensitivity to EUC changes overwhelming other important processes like diffusion and biology. This shortcoming compromises the ability to reproduce the OMZ variability and could explain the disparate trends in ESMs projections.

Plain Language Summary We expect an expansion of the ocean low-oxygen areas as the climate warms. This expansion would bring low-oxygen waters closer to the ocean surface in the Pacific Ocean and affect the global uptake of carbon and interactions between marine animals. We show that commonly used low-resolution climate models misrepresent characteristics of one of the major ocean currents—the Equatorial Undercurrent—with implications for the depth of the low-oxygen waters. Using a higher-resolution climate model we refine the representation of the Equatorial Undercurrent and the low-oxygen areas in the equatorial Pacific. We postulate that shortcomings of low-resolution models compromise our ability to reproduce areas of low oxygen and their response to climate change.

1. Introduction

As the global ocean warms (Cheng et al., 2017; Johnson et al., 2018; Resplandy et al., 2018), it loses oxygen to the atmosphere mostly due to decreased solubility and reduced ventilation (Helm et al., 2011; Keeling et al., 2010; Levin, 2018; Long et al., 2016; Schmidtko et al., 2017). In response to this global deoxygenation, subsurface oxygen minimum zones (OMZs) are expected to expand, bringing very low oxygen waters closer to the ocean surface (Oschlies et al., 2008). These changes in the depth of the OMZ upper boundary could have severe impacts on marine life and biogeochemical cycling (Gruber, 2004; Levin, 2018), such as the compression of the habitat of commercially fished species and related ecosystems (Chu & Tunnicliffe, 2015; Sperling et al., 2013; Stramma et al., 2012), the reduction of carbon export by migrating zooplankton (Bianchi et al., 2013), and the release of nitrous oxide to the atmosphere (Arévalo-Martínez et al., 2015; Babbin et al., 2015; Ji et al., 2018; Yang et al., 2017).

In the Pacific Ocean, observations and models show disparate trends in the OMZ volume. Observations suggest that the OMZ expanded over the past 50 years (Stramma et al., 2008), while studies based on isotopes from sediment cores suggest that multidecadal to centennial fluctuations in the vertical extent of the OMZ could obscure long-term anthropogenic trends in shorter observational records (Deutsch et al., 2014). Coarse ($\mathcal{O}$ 1° horizontal resolution) ESMs show strong disagreement in the sign of change in OMZ volume by year 2100 (from −15% to +15% for 1960–2100) (Bopp et al., 2013; Cabré et al., 2015), and on longer time scales with some models suggesting that OMZs might shrink after their initial expansion (Fu et al., 2018).

OMZs are controlled by a delicate balance between the rate of biological consumption of oxygen during remineralization and denitrification processes, and the supply of oxygen by air-sea exchange and ocean ventilation. Models robustly project a decrease in oxygen caused by warming-induced changes in solubility and

an increase in oxygen due to reduced biological production and respiration in OMZs (Cabré et al., 2015; Bopp et al., 2013, 2017). However, there is no consensus on the spatial and temporal changes in ventilation and their impact on the volume of OMZs (Fu et al., 2018; Resplandy, 2018; Shigemitsu et al., 2017).

The ocean is ventilated by advective and diffusive processes. Advection redistributes water masses in the ocean (e.g., Busecke et al., 2017) and can influence local oxygen concentrations by reshaping the OMZ and changing the position of its boundaries (Czeschel et al., 2010, 2015; Stramma et al., 2010). In contrast, eddy diffusion can influence the volume of the OMZ by supplying oxygen and balancing biological consumption in the OMZ (Brandt et al., 2015; Gnanadesikan et al., 2013). Coarse ESMs suggest that the Equatorial Undercurrent (EUC) is one of the largest sources of forced variability and model uncertainty in the projected changes in the OMZ (Shigemitsu et al., 2017). Models which project a weakening of the EUC also tend to project an expansion of the OMZ in the equatorial band and vice versa. A common bias of these coarse resolution models, however, is that they do not resolve the complex dynamics of the EUC; specifically, they do not represent the narrow alternating currents observed close to the equator (e.g., Kessler, 2006) and the EUC in these models is generally too wide and too weak (Cabré et al., 2015).

Here we examine the tropical Pacific OMZ response to EUC dynamics. We show that the structure of the EUC controls the geometry and variability of the upper OMZ by contrasting a coarse ESM with an eddying ESM that reproduces key observed features of the EUC. The wide and weak EUC simulated by coarse models yields an unrealistic "tilt" of the upper OMZ boundary, which exacerbates its sensitivity to temporal changes and has implications for projections of the OMZ volume.

2. Methods

We define OMZs as areas with oxygen concentration lower than 80 μmol/kg and the OMZ boundary as the surface of 80-μmol/kg concentration. This manuscript focuses on the upper OMZ boundary, hence throughout the manuscript we refer to the upper boundary as "OMZ boundary" for brevity. The tilt and "depth" of the OMZ boundary are defined as the slope and intercept of a linear regression (see supporting information).

2.1. EUC Characterization

We define the EUC based on the positive zonal velocity u in the upper 500 m of the water column. Several key metrics are derived from zonal velocity averages between 1°S and 1°N (details in the supporting information):

1. *EUC core*: depth of maximum u.
2. *EUC boundary*: the contour of u equal to 0.2 m/s.
3. *EUC thickness*: the distance between the upper and lower EUC boundary.

The tilt of the lower EUC boundary is defined identical to the OMZ tilt as the slope of the linear regression on the boundary (see supporting information).

2.2. Models

We use the Geophysical Fluid Dynamics Laboratory (GFDL) coupled models of the CM2-O suite, which include the same atmospheric, ice, and land components. For the ocean, each simulation has identical vertical grid configurations and parametrizations of vertical mixing processes but different horizontal resolution and horizontal parameterizations (Delworth et al., 2011; Griffies et al., 2015). We use the nominal 1° configuration CM2.1deg, referred to as the "coarse" model, and the nominal 1/10° CM2.6 referred to as the "eddying" model. The neutral tracer diffusion coefficient in CM2.1deg is 600 m^2/s and the diffusion coefficient, used to parameterize eddy advection, varies between 100 and 1,200 m^2/s as a function of the flow field (see Griffies et al., 2015 for details). CM2.6 does not include parameterizations of neutral diffusion or eddy advection. Both models include the simplified biogeochemical module "miniBling" with three prognostic tracers (Galbraith et al., 2015). We use preindustrial simulations forced by a constant atmospheric CO_2 concentrations of 286 ppm and initialized with identical observed initial conditions (Dufour et al., 2015). The circulation is spun up from rest and run for a total of 200 years. The biogeochemical module is started in year 48. For this study we analyze the last 20 years (181–200). We decompose the oxygen budget into dynamical and biological contributions (supporting information), including large-scale advection, vertical diffusion, and eddy effects (parameterized and resolved depending on the model resolution).

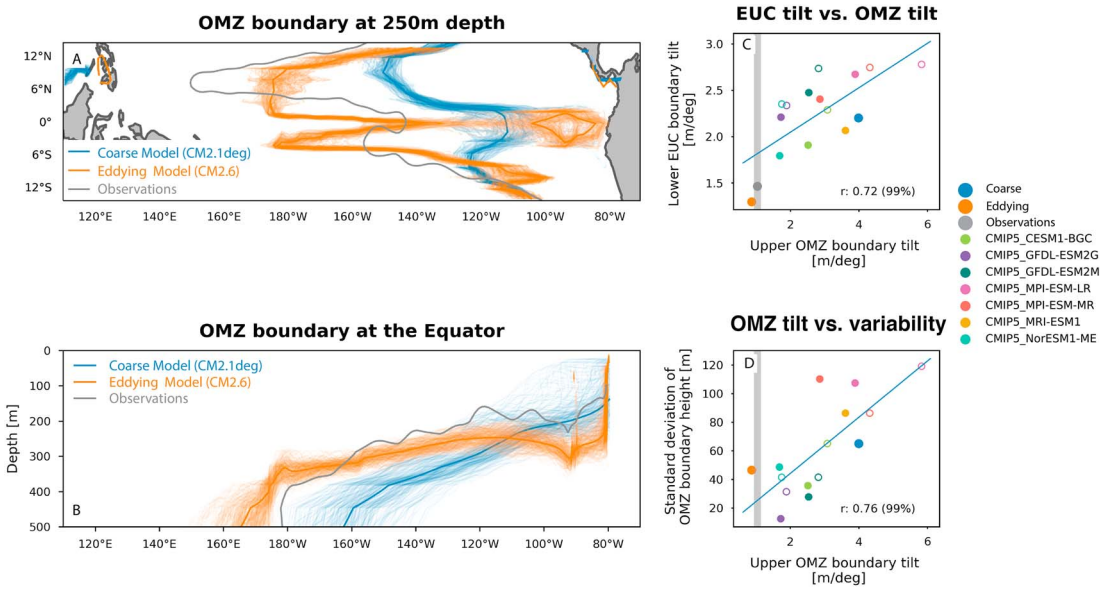

Figure 1. (a) Position of the oxygen minimum zones (OMZ) boundary (80 μmol/kg) at 250 m in the coarse model (blue), the eddying model (orange), and the observations (black; Bianchi et al., 2012). Thick lines represent long-term averages (20 years for models), and thin lines indicated monthly values. The eddying model is box-averaged on a ~2° by 2° grid (20(eddying)/4(coarse) grid cells in each direction), to enable comparison with the gridded observations. (b) Position of the OMZ boundary along the equator, based on values averaged from 1°S to 1°N (colors as in Figure 1a). (c) Relationship between the OMZ boundary tilt and lower equatorial Undercurrent (EUC) boundary tilt in observations, CM2-O coarse and eddying models, and CMIP5 piControl runs (filled symbols) and RCP8.5 runs (open symbols). (d) As in (c) but for the relationship between the tilt and the standard deviation of the OMZ upper boundary depth (see supporting information for details). In (c) and (d), the gray bar indicates the observed OMZ boundary tilt.

Additionally, we analyze a subset of the Coupled Model Intercomparison Project 5 (CMIP5) models (Taylor et al., 2011). We use 20 years annual output of preindustrial (piControl; last 20 years of each run) and business as usual (RCP8.5; 2081–2100) simulations (supporting information). Most of the CMIP models have a comparable resolution to the coarse model CM2.1deg described above, but throughout the text "coarse model" will exclusively refer to CM2.1deg. The neutral diffusivity coefficients for the CMIP5 models range from 500–1,000 m^2/s (Cabré et al., 2015).

Different spin-up strategies (200 years for CM2-O models and 1,000-10,000 years for CMIP5 models) could influence the OMZ, but are likely to influence the deeper regions in the Eastern Pacific rather than the upper boundary, which equilibrates on much faster time scales (Séférian et al., 2016).

2.3. Observations

In this study we use the oxygen climatology by Bianchi et al. (2012). For velocity observations we use optimally interpolated Shipboard Acoustic Doppler Current Profiler (ADCP) data from Johnson et al. (2002), derived from 172 ship sections taken throughout the 1990s, providing a decadal view of the EUC.

3. Results

3.1. OMZ Geometry

The observed zonal extent of the upper OMZ in the Equatorial Pacific varies between 150°E at 5°N and 140°W at the equator (Figure 1a). Despite these strong east-west excursions linked to the presence of alternating jets in the equatorial current system, the OMZ upper boundary at a given latitude lays at a relatively constant depth. Around the equator, the boundary is located at 200- to 300-m depth east of 180°W where it sharply deepens to more than 500 m (Figure 1b). The boundary is also characterized by a depression associated with the Galapagos Islands (90°W).

The eddying model reproduces observed characteristics of the OMZ boundary, including strong east-west excursions, a flat boundary shape and the Galapagos Islands depression; although the OMZ is slightly too deep in the eastern Pacific (Figures 1a and 1b). In the coarse model, the OMZ is confined to the east, and the boundary shows considerably less zonal structure and a much larger tilt (i.e., deepening from 200 m at 90°W down to 500 m at 180°W) than observations (Figures 1a and 1b) and is missing the depression

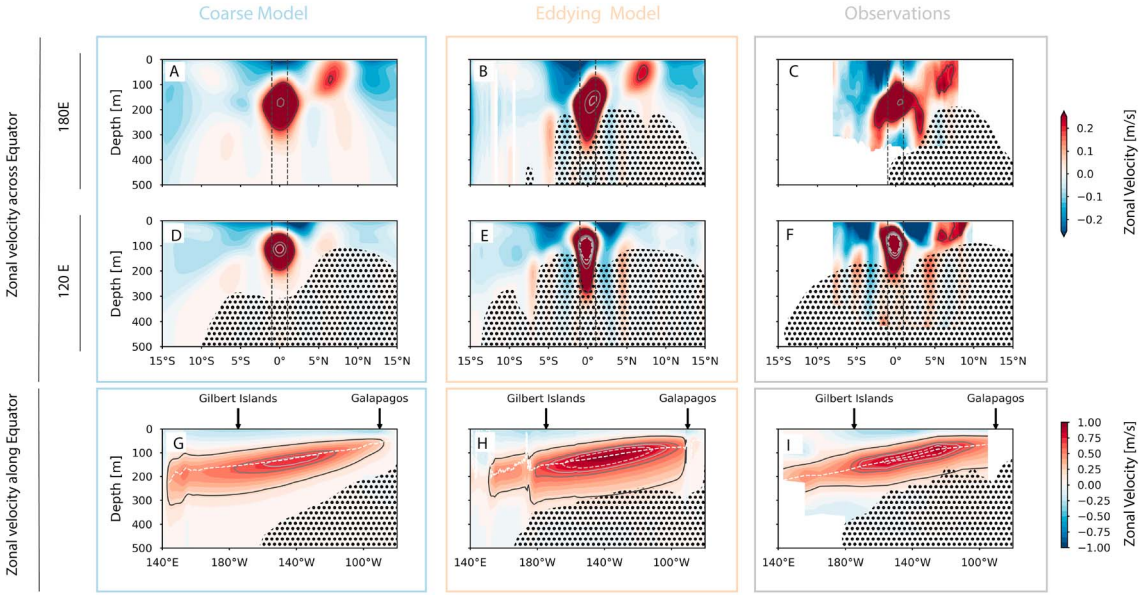

Figure 2. Comparison of zonal velocities (color) and oxygen minimum zones (dotted area: values <80 μmol/kg) between the coarse model (left column), the eddying model (middle column), and observations from Johnson et al. (2002) and Bianchi et al. (2012) (right column). (a–f) Zonal velocity across the equator are shown at 180°W (a–c) and 125°W (d–f). Dashed lines show the position of 1°S and 1°N. (g–i) Zonal velocity averaged between 1°S to 1°N. The depth of the EUC core is shown (white dashed). Contours indicate velocities of 20, 60, 70, and 80 cm/s (light gray) and the EUC core (white-dashed).

feature around the Galapagos. The observations do not resolve the interannual variability in the OMZ but the eddying model suggests that the depth of the upper OMZ varies by less than ~50 m interannually while the coarse model shows year-to-year variations larger than ~150 m (Figure 1b).

This OMZ tilt is of the order of 1 m/deg in the observations, 0.8 m/deg in the eddying model, but about 5 m/deg in the coarse model (Figures 1c and 1d). Combining our two models with a suite of seven CMIP5 models, we find that coarse resolution ESMs systematically overestimate the OMZ tilt, with simulated values ranging from 1.5 and 6 m/deg (Figures 1c and 1d; see also Figure S5 in the supporting information) and that models with stronger OMZ tilts are also models in which the upper OMZ is more variable on interannual time scales (Figure 1d). The magnitude of the OMZ tilt is closely related to the geometry of the EUC, specifically the tilt of the lower EUC (Figure 1c). This suggests that the geometry and the variability of the upper OMZ are tightly linked to the EUC dynamics.

3.2. EUC Dynamics Influence Its Geometry

Observations show that the EUC is narrow (2°S to 2°N) and flanked by distinct "off-equatorial" currents, including the eastward Subsurface Counter Currents or Tsuchiya jets (at 150–400 m depth and 5°N/S) and the westward North and South Equatorial Intermediate Currents (at 200- to 400-m depth and 3°N/S) (Figure 2f, and, e.g., Stramma et al., 2010). The eddying model reproduces the narrow EUC and the high velocities within its core, while the coarse model produces a significantly weaker and wider EUC, extending from 3°S to 3°N. The eddying model also reproduces the vertical shape and position of the 'off-equatorial' currents but their intensity is generally too weak compared to observations (Figures 2e and 2f). In contrast, the coarse model fails to simulate these alternating "off-equatorial" currents (Figure 2d), similarly to CMIP5 models (Cabré et al., 2015).

Observations also show that the EUC maintains a relatively uniform thickness (vertical extent) of 100- to 150-m depth across the whole Pacific basin (Figure 2i). The core of the EUC shallows from ~200 m in the west to ~60 m in the east (Figure 2i, Figures S3 and S4). It is most intense at the center of the basin, between the Gilbert Islands (175°W) and the Galapagos Islands (90°W) where the velocity exceeds 0.5 m/s and reaches up to 1 m/s (Figure 2i). Both models reproduce the eastward shallowing of the EUC core. Only the eddying model reproduces the intense velocities >0.5 m/s between the two island groups and the uniform thickness across the basin, although both peak velocities and thickness slightly exceed what is observed. In contrast, the EUC in the coarse model rapidly slows down ($u < 0.5$ m/s east of 120°W) and its thickness

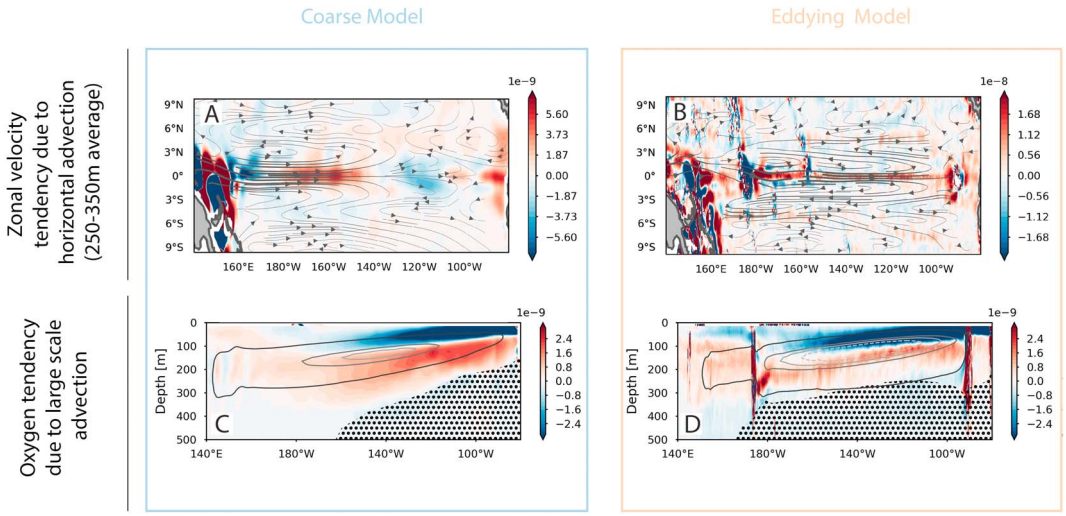

Figure 3. (a,b) Changes in zonal velocity due to horizontal advection averaged between 250- and 350-m depth in the coarse (a) and eddying (b) models (m s^{-2}). Regions of enhanced (reduced) zonal velocity are in red (blue). Note the different colorbars. Gray lines and arrows illustrate the horizontal circulation in the domain; line thickness scales with the velocity amplitude. (c,d) Changes in oxygen concentrations due to large-scale advection at the equator (1°S to 1°N average) in the coarse (c) and eddying (d) models (mol kg^{-1} s^{-1}). Oxygen supply is positive (red). Contours indicate mean zonal velocity and the dotted area the oxygen minimum zones like in Figure 2. For details on the calculation of the budget terms see (supporting information).

reduces from ~200 m in the west to <100 m in the east, following the shallowing of the EUC lower boundary (Figure 2g; supporting information).

Differences in the EUC shape, in particular, the thickness, are tied to fundamental differences in the equatorial circulation between the two models (Figures 3a/3b). In the eddying model, the zonal jets generate an intense zonal recirculation that largely keeps equatorial waters confined between 5°S and 5°N. In the coarse model, however, the equatorial horizontal circulation diverges in the eastern Pacific, exporting waters into the subtropical gyre circulation (see eastern Pacific in Figure 3a). As a result, the horizontal circulation reinforces the flow of the lower EUC in the eddying model (Figure 3b). In the coarse model, the horizontal circulation reinforces the lower EUC flow only in the western Pacific and slows it down in the eastern Pacific (Figure 3a). This divergence of the horizontal flow explains the strong tapering off of the EUC, and the presence of a shallower and more tilted lower EUC boundary in the eastern Pacific in the coarse model (Figure 2g).

3.3. Dynamical Control of OMZ

The mean structure of the upper OMZ follows the dynamical structure of the lower EUC. In the observations and the eddying model, the OMZ boundary aligns with the relatively flat shape of the lower EUC boundary (Figures 2h and 2i) and deepens around the Galapagos Islands, indicating a local increase in oxygen concentrations. This local feature is likely due to the interaction between the strong current and the blocking landmasses (Karnauskas et al., 2010). In the coarse model, however, the OMZ boundary follows the strong tilt of the lower EUC boundary and crosses isopycnals as it shallows eastward (not shown).

Mechanistically, the link between EUC and OMZ geometry is dominated by large-scale transport patterns. In both models, it is the advection that controls the shape of the upper OMZ (depth and tilt), by supplying oxygen above the OMZ and limiting its expansion toward the surface (Figures 3c and 3d). Eddy effects supply oxygen over most of the region, both in the OMZ and above, and are therefore less important for the position of the upper OMZ (Figures S6e–S6h). Note that in the eddying model, the supply of oxygen by vertical diffusion explains the Galapagos depression, but is weak elsewhere (Figure S6j). Other processes are too weak (submesoscale, Figure S6k/S6l) or of opposed sign (biological consumption; Figures S6a/S6b).

3.4. Temporal Variability in the OMZ Boundary

The temporal variability of the upper OMZ depends on its mean tilt (Figure 1d). This can be understood by considering the OMZ response to changes in zonal flow. A change in the zonal flow will have little effect

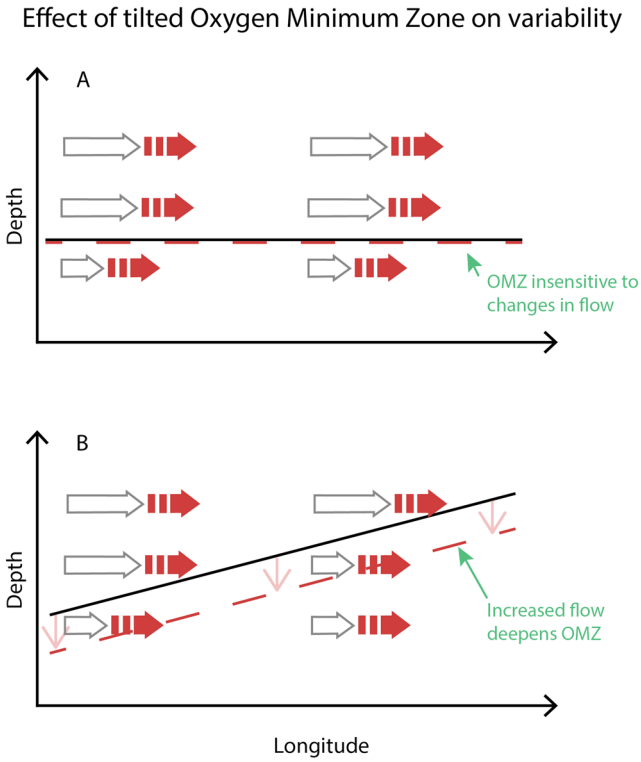

Figure 4. Influence of mean OMZ tilt on temporal variability. Panel (a) shows a oxygen minimum zone (OMZ) boundary (black line) that is oriented parallel to the flow (gray arrows). Changes in the flow (red arrows) do not influence the height of the OMZ boundary (red dashed line). Panel (b) contrasts this picture with a tilted OMZ (black line) due to a different mean flow structure (gray arrows). A similar change (increase) in flow as in (a) will move the OMZ boundary (red dashed line) and thus lower the boundary locally (red thin arrows).

on the depth of a surface if this surface is parallel to the flow direction (Figure 4a). In contrast, variations in the zonal flow will move the surface zonally if this surface is slanted relative to the flow and lead to vertical variations of the surface (deepening for increased eastward flow and shallowing for decreased flow, Figure 4b). A tilted OMZ is therefore more sensitive to changes in zonal flow and is more likely to exhibit strong temporal variations in the depth of its boundary (Figure 4).

We focus here on the strong interannual variability of the zonal velocity. According to an EOF analysis of the zonal velocity, coarse and eddying models show similar patterns of interannual temporal variability, which can be decomposed in two modes:

1. A "surface" mode characterized by a weaker westward surface current (positive anomalies), a weaker EUC in the west (negative anomalies), and a stronger EUC in the east (positive anomalies, Figures 5a/5b). This mode leads the temperature-based NINO 3.4 index by 2–3 months, suggesting that it is related to changes in the wind field preceding El Niño-Southern Oscillation events.
2. A "shoaling" mode, characterized by higher velocities above the EUC core and lower velocities below the EUC core (i.e., an upward shift of the EUC), which is correlated with basin-wide changes in the thermocline tilt (pink lines in Figure 5). This mode lags the NINO3.4 index by about 6 months in both models (Figures 5c/5d).

These two modes are reproduced similarly in both models, but the response of the OMZ is very different in each case. In the coarse model, the dominant mode of oxygen variability is correlated to the shoaling mode that lifts the OMZ boundary as the lower EUC weakens (see black lines in Figure 5c and supporting information). The surface mode only yields a slight deepening confined east of 100°W (black lines in Figure 5a). In the eddying model, however, the impact of both modes on the OMZ is very limited (black lines in Figures 5b and 5d). This is consistent with the simple mechanism proposed above: a flatter OMZ is less sensitive to changes in zonal flow (Figure 4). Hence, the differences in the mean OMZ shape (tilt) have far reaching implications for the OMZ response to dynamical variability. In the coarse model, interannual vari-

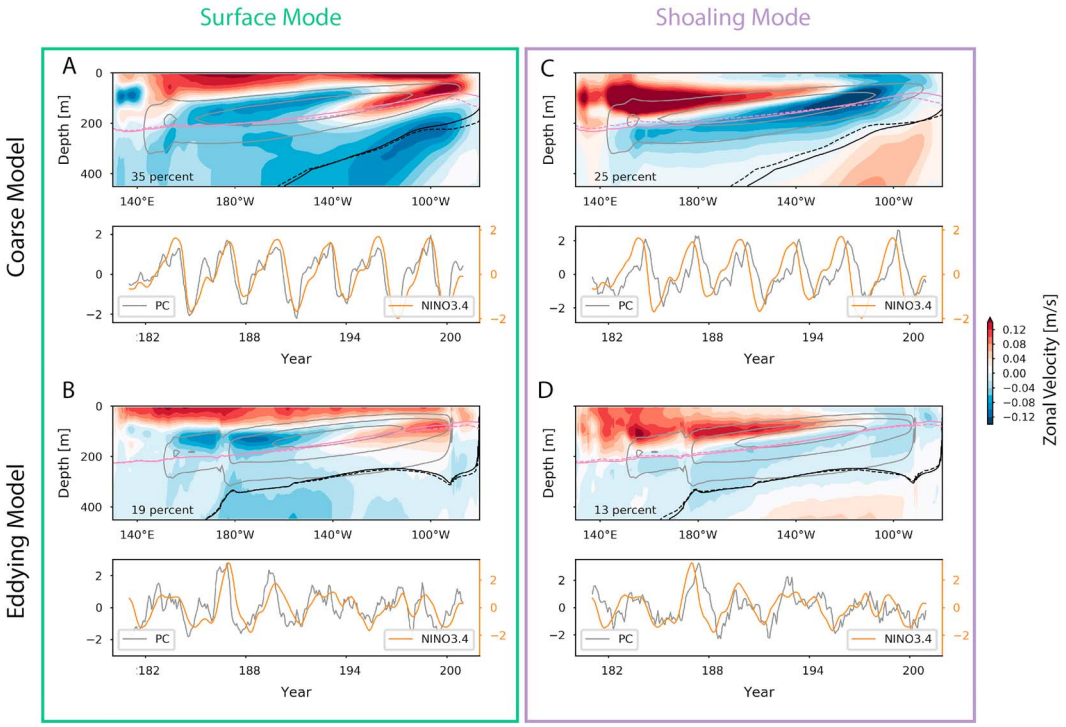

Figure 5. (a–d) The two dominant EOF modes of interannual variability in zonal velocity along the equator (1°S to 1°N average) in the coarse model (a/c) and the eddying model (b/d), which are referred to as the "surface" mode (left) and "shoaling" mode (right). Each panel shows the EOF pattern in colors (m/s), the mean shape of the EUC as gray contours (same as Figure 2), the 1,026.0 kg m^{-3} density surface in pink, and the OMZ boundary in black. Solid contours indicate mean fields (OMZ boundary, etc.), and dashed contours indicate the change associated with each mode (i.e., fields regressed onto the principal component (PC) of the mode shown). The percentage of the total variance explained by each mode is shown in the lower left. Time series show the temporal evolution of the principal component for each mode (gray line) and the NINO3.4 index (orange). For more details on the method, see supporting information.

ations in large-scale zonal velocities control the OMZ variability and overwhelm other process like diffusion and biology (Figure S7). In the eddying model, the OMZ variability is weaker (Figure 1) and controlled by both large-scale advection and eddy effects (see Figure S7d/S7f).

These findings are not exclusive to the two models examined in detail in this study. Most coarse CMIP5 models share the same underlying bias in the shape of the EUC and the OMZ (tilt in Figure 1c). Our results suggest that this bias likely amplifies the response of the OMZ to EUC changes, leading to an exaggerated shallowing or deepening of the OMZ for a given change in the EUC.

4. Discussion

We investigated how the equatorial circulation affects the upper OMZ in the Pacific in a suite of ESMs. Our results show that the Equatorial Undercurrent (EUC) controls the position and variability of the upper OMZ in this region. All low-resolution ESMs considered here systematically show a thinning of the EUC in the eastern Pacific. In the low-resolution model we examined in detail ("coarse"), this thinning of the EUC is explained by a strong divergence of the zonal equatorial flow and a loss of waters to the subtropical gyre circulation. In contrast, the presence of zonally alternating jets in the high-resolution model ("eddying") confines the horizontal circulation close to the equator and yields a faster EUC of relatively uniform thickness across the basin.

The representation of the EUC circulation has major implications for the OMZ mean state. The EUC determines the shape and depth of the OMZ boundary along the equator. A more uniform thickness in the EUC leads to a flatter OMZ boundary, as seen in the observations and the eddying model. The OMZ depth directly influences key biological processes, such as the remineralization depth (Deutsch et al., 2014), the amplitude of zooplankton vertical migration (Bianchi et al., 2013) and the rate of denitrification (Yang et al., 2017). Fur-

thermore, the large east-west OMZ excursions associated with the zonal jets in the EUC system (Figure 1a) increase the surface to volume ratio of the OMZ and are therefore likely to promote eddy diffusion, which is the major source of oxygen in the OMZ (Brandt et al., 2015; Gnanadesikan et al., 2013; Palter & Trossman, 2018).

The mean shape of the OMZ subsequently influences its interannual variability. Models with unrealistically tilted OMZ are too sensitive to changes in zonal flow and show strong interannual variations in the depth of their upper boundary. The interannual changes in the EUC highlighted in this study show spatial patterns comparable to the long-term changes expected from CMIP3 models (see Figure 1 in Gupta et al., 2012). The relationship found between OMZ tilt and OMZ sensitivity to EUC changes is therefore likely to be relevant in the context of forced climatic changes. Shigemitsu et al. (2017) showed that the changes in OMZ volume simulated in CMIP5 models were tied to the changes in EUC transport simulated in each model (weaker EUC yields smaller OMZ and vice versa). These models all share the same underlying bias in the shape of the OMZ, which likely amplifies this influence of the EUC. This suggests that models with a more realistic and flat OMZ would be less sensitive to long-term changes in EUC. Improving the representation of the EUC appears a necessary step to improve projections of the OMZ and possibly reconcile models disparate future trends. In this study, we showed the importance of the EUC mean state and temporal variability for the OMZ, but the existence of systematic biases in the circulation is also relevant in the context of heat (Coats & Karnauskas, 2018) and nutrients (Qin Xuerong et al., 2016) transport to the equatorial Pacific and "downstream" regions like the Peruvian coast (Montes et al., 2010; Espinoza-Morriberón et al., 2017).

Acknowledgments
Code and data to reproduce the results of this study are provided in Zenodo archives (https://zenodo.org/record/3236505, https://zenodo.org/record/2648855). We acknowledge the World Climate Research Programme's Working Group on Coupled Modelling, which is responsible for CMIP, and we thank the climate modeling groups (Table S1 in the supporting information.) for producing and making available their model output. For CMIP the U.S. Department of Energy's Program for Climate Model Diagnosis and Intercomparison provides coordinating support and led development of software infrastructure in partnership with the Global Organization for Earth System Science Portals. We thank Graeme McGilchrist, Xiao Liu, Jong-Yeon Park, and the two anonymous reviewers for their thoughtful comments which greatly improved the manuscript. This research was funded under the NOAA Cooperative Institute for Climate Science agreement NA14OAR4320106.

References

Arévalo-Martínez, D. L., Kock, A., Löscher, C. R., Schmitz, R. A., & Bange, H. W. (2015). Massive nitrous oxide emissions from the tropical South Pacific Ocean. *Nature Geoscience*, *8*(7), 530–533. Retrieved 2019-01-17TZ, from https://www.nature.com/articles/ngeo2469, https://doi.org/10.1038/ngeo2469

Babbin, A. R., Bianchi, D., Jayakumar, A., & Ward, B. B. (2015). Rapid nitrous oxide cycling in the suboxic ocean. *Science*, *348*(6239), 1127–1129. http://www.sciencemag.org/cgi/doi/10.1126/science.aaa8380, https://doi.org/10.1126/science.aaa8380

Bianchi, D., Dunne, J. P., Sarmiento, J. L., & Galbraith, E. D. (2012). Data-based estimates of suboxia, denitrification, and N_2O production in the ocean and their sensitivities to dissolved O_2. *Global Biogeochemical Cycles*, *26*, GB2009. https://doi.org/10.1002/gbc.20031

Bianchi, D., Galbraith, E. D., Carozza, D. A., Mislan, K. A. S., & Stock, C. A. (2013). Intensification of open-ocean oxygen depletion by vertically migrating animals. *Nature Geoscience*, *6*(7), 545–548. Retrieved 2019-01-30TZ, from http://www.nature.com/articles/ngeo1837, https://doi.org/10.1038/ngeo1837

Bianchi, D., Stock, C., Galbraith, E. D., & Sarmiento, J. L. (2013). Diel vertical migration: Ecological controls and impacts on the biological pump in a one-dimensional ocean model. *Global Biogeochemical Cycles*, *27*, 478–491. http://doi.org/10.1002/gbc.20031

Bopp, L., Resplandy, L., Orr, J. C., Doney, S. C., Dunne, J. P., Gehlen, M., et al. (2013). Multiple stressors of ocean ecosystems in the 21st century: projections with CMIP5 models. *Biogeosciences*, *10*, 3627–3676. https://doi.org/10.5194/bg-10-6225-2013

Bopp, L., Resplandy, L., Untersee, A., Le Mezo, P., & Kageyama, M. (2017). Ocean (de)oxygenation from the Last Glacial Maximum to the twenty-first century: Insights from Earth System models. *Philosophical Transactions of the Royal Society A: Mathematical, Physical and Engineering Sciences*, *375*(2102), 20160323. http://rsta.royalsocietypublishing.org/lookup/doi/10.1098/rsta.2016.0323, https://doi.org/10.1098/rsta.2016.0323

Brandt, P., Bange, H. W., Banyte, D., Dengler, M., Didwischus, S.-H., Fischer, T., et al. (2015). On the role of circulation and mixing in the ventilation of oxygen minimum zones with a focus on the eastern tropical North Atlantic. *Biogeosciences*, *12*(2), 489–512. Retrieved 2018-07-24TZ https://www.biogeosciences.net/12/489/2015/, https://doi.org/10.5194/bg-12-489-2015

Busecke, J., Abernathey, R. P., & Gordon, A. L. (2017). Lateral eddy mixing in the subtropical salinity maxima of the Global Ocean. *Journal of Physical Oceanography*, *47*(4), 737–754. Retrieved 2017-11-30TZ, from http://journals.ametsoc.org/doi/abs/10.1175/JPO-D-16-0215.1, https://doi.org/10.1175/JPO-D-16-0215.1

Cabré, A., Marinov, I., Bernardello, R., & Bianchi, D. (2015). Oxygen minimum zones in the tropical Pacific across CMIP5 models: mean state differences and climate change trends. *Biogeosciences*, *12*(18), 5429–5454. Retrieved 2018-05-31TZ, from http://www.biogeosciences.net/12/5429/2015/, https://doi.org/10.5194/bg-12-5429-2015

Cheng, L., Trenberth, K. E., Fasullo, J., Boyer, T., Abraham, J., & Zhu, J. (2017). Improved estimates of ocean heat content from 1960 to 2015. *Science Advances*, *3*(3), e1601545. Retrieved 2018-09-13TZ, from http://advances.sciencemag.org/content/3/3/e1601545, https://doi.org/10.1126/sciadv.1601545

Chu, J. W. F., & Tunnicliffe, V. (2015). Oxygen limitations on marine animal distributions and the collapse of epibenthic community structure during shoaling hypoxia. *Global Change Biology*, *21*(8), 2989–3004. Retrieved 2019-01-17TZ, from https://onlinelibrary.wiley.com/doi/abs/10.1111/gcb.12898, https://doi.org/10.1111/gcb.12898

Coats, S., & Karnauskas, K. B. (2018). A role for the Equatorial Undercurrent in the ocean dynamical thermostat. *Journal of Climate*. Retrieved 2018-06-22TZ, from https://journals.ametsoc.org/doi/abs/10.1175/JCLI-D-17-0513.1, https://doi.org/10.1175/JCLI-D-17-0513.1

Czeschel, R., Stramma, L., Schwarzkopf, F. U., Giese, B. S., Funk, A., & Karstensen, J. (2010). Middepth circulation of the eastern tropical South Pacific and its link to the oxygen minimum zone. *Journal of Geophysical Research*, *116*, C01015. https://doi.org/10.1029/2010JC006565

Czeschel, R., Stramma, L., Weller, R. A., & Fischer, T. (2015). Circulation, eddies, oxygen, and nutrient changes in the eastern tropical South Pacific Ocean. *Ocean Science*, *11*(3), 455–470. Retrieved 2018-07-03TZ, from https://www.ocean-sci.net/11/455/2015/, https://doi.org/10.5194/os-11-455-2015

Delworth, T. L., Rosati, A., Anderson, W., Adcroft, A. J., Balaji, V., Benson, R., et al. (2011). Simulated climate and climate change in the GFDL CM2.5 high-resolution coupled climate model. *Journal of Climate*, *25*(8), 2755–2781. Retrieved 2018-06-20TZ, from https://journals.ametsoc.org/doi/abs/10.1175/JCLI-D-11-00316.1, https://doi.org/10.1175/JCLI-D-11-00316.1

Deutsch, C., Berelson, W., Thunell, R., Weber, T., Tems, C., McManus, J., et al. (2014). Centennial changes in North Pacific anoxia linked to tropical trade winds. *Science*, *345*(6197), 665–668. Retrieved 2017-12- 04TZ from http://science.sciencemag.org/content/345/6197/665, https://doi.org/10.1126/science.1252332

Dufour, C. O., Griffies, S. M., de Souza, G. F., Frenger, I., Morrison, A. K., Palter, J. B., et al. (2015). Role of mesoscale eddies in cross-frontal transport of heat and biogeochemical tracers in the Southern Ocean. *Journal of Physical Oceanography*, *45*(12), 3057–3081. Retrieved from http://journals.ametsoc.org/doi/abs/10.1175/JPO-D-14-0240.1%5Cn, https://doi.org/10.1175/JPO-D-14-0240.1

Espinoza-Morriberón, D., Echevin, V., Colas, F., Tam, J., Ledesma, J., Vásquez, L., & Graco, M. (2017). Impacts of El Niño events on the Peruvian upwelling system productivity. *Journal of Geophysical Research: Oceans*, *122*, 5423–5444. https://doi.org/10.1002/2016JC012439

Fu, W., Primeau, F., Keith Moore, J., Lindsay, K., & Randerson, J. T. (2018). Reversal of increasing tropical ocean hypoxia trends with sustained climate warming. *Global Biogeochemical Cycles*, *32*, 551–564. http://doi.org/10.1002/2017GB005788

Galbraith, E. D., Dunne, J. P., Gnanadesikan, A., Slater, R. D., Sarmiento, J. L., Dufour, C. O., et al. (2015). Complex functionality with minimal computation: Promise and pitfalls of reduced-tracer ocean biogeochemistry models. *Journal of Advances in Modeling Earth Systems*, *7*, 2012–2028. https://doi.org/10.1002/2015MS000463

Gnanadesikan, A., Bianchi, D., & Pradal, M.-A. (2013). Critical role for mesoscale eddy diffusion in supplying oxygen to hypoxic ocean waters. *Geophysical Research Letters*, *40*, 5194–5198. https://doi.org/10.1002/grl.50998

Griffies, S. M., Winton, M., Anderson, W. G., Benson, R., Delworth, T. L., Dufour, C. O., et al. (2015). Impacts on ocean heat from transient mesoscale eddies in a hierarchy of climate models. *Journal of Climate*, *28*(3), 952–977. Retrieved 2018-01-31TZ, from http://journals.ametsoc.org/doi/10.1175/JCLI-D-14-00353.1. https://doi.org/10.1175/JCLI-D-14-00353.1

Gruber, N. (2004). The dynamics of the marine nitrogen cycle and its influence on atmospheric co2 variations. In M. Follows, & T. Oguz (Eds.), *The Ocean Carbon Cycle and Climate* (pp. 97–148). Dordrecht: Springer Netherlands. Retrieved 2019-01-17TZ, from http://link.springer.com/10.1007/978-1-4020-2087-2_4, https://doi.org/10.1007/978-1-4020-2087-2_4

Gupta, A. S., Ganachaud, A., McGregor, S., Brown, J. N., & Muir, L. (2012). Drivers of the projected changes to the Pacific Ocean equatorial circulation. *Geophysical Research Letters*, *39*, L09605. https://doi.org/10.1029/2012GL051447

Helm, K. P., Bindoff, N. L., & Church, J. A. (2011). Observed decreases in oxygen content of the global ocean. *Geophysical Research Letters*, *38*, L23602. https://doi.org/10.1029/2011GL049513

Ji, Q., Buitenhuis, E., Suntharalingam, P., Sarmiento, J. L., & Ward, B. B. (2018). Global nitrous oxide production determined by oxygen sensitivity of nitrification and denitrification. *Global Biogeochemical Cycles*, *32*, 1790–1802. https://doi.org/10.1029/2018GB005887

Johnson, G. C., Lyman, J. M., Boyer, T., Cheng, L., Domingues, C. M., Gilson, J., et al. (2018). Ocean Heat content, *State of the Climate in 2017*.Boston, MA: American Meteorological Society.

Johnson, G. C., Sloyan, B. M., Kessler, W. S., & McTaggart, K. E. (2002). Direct measurements of upper ocean currents and water properties across the tropical Pacific during the 1990s. *Progress in Oceanography*, *52*(1), 31–61. Retrieved 2018-05-02TZ, from http://linkinghub.elsevier.com/retrieve/pii/S0079661102000216, https://doi.org/10.1016/S0079-6611(02)00021-6

Karnauskas, K. B., Murtugudde, R., & Busalacchi, A. J. (2010). Observing the Galápagos–EUC interaction: Insights and challenges. *Journal of Physical Oceanography*, *40*(12), 2768–2777. Retrieved 2018-08-07TZ, from https://doi.org/10.1175/2010JPO4461.1

Keeling, R. F., Körtzinger, A., & Gruber, N. (2010). Ocean deoxygenation in a warming world. *Annual Review of Marine Science*, *2*(1), 199–229. Retrieved 2018-01-22TZ, from https://doi.org/10.1146/annurev.marine.010908.163855

Kessler, W. S. (2006). The circulation of the eastern tropical Pacific: A review. *Progress in Oceanography*, *69*(2), 181–217. Retrieved 2018-07-26TZ, from http://www.sciencedirect.com/science/article/pii/S0079661106000310, https://doi.org/10.1016/j.pocean.2006.03.009

Levin, L. A. (2018). Manifestation, drivers, and emergence of open ocean deoxygenation. *Annual Review of Marine Science*, *10*(1), 229–260. Retrieved 2018- 02-08TZ, from https://doi.org/10.1146/annurev-marine-121916-063359

Long, M. C., Deutsch, C., & Ito, T. (2016). Finding forced trends in oceanic oxygen: Trends in dissolved oxygen. *Global Biogeochemical Cycles*, *30*, 381–397. http://doi.org/10.1002/2015GB005310

Montes, I., Colas, F., Capet, X., & Schneider, W. (2010). On the pathways of the equatorial subsurface currents in the eastern equatorial Pacific and their contributions to the Peru-Chile Undercurrent. *Journal of Geophysical Research*, *115*, C09003. http://doi.org/10.1029/2009JC005710

Oschlies, A., Schulz, K. G., Riebesell, U., & Schmittner, A. (2008). Simulated 21st century's increase in oceanic suboxia by CO_2 -enhanced biotic carbon export: Rapid increase in oceanic suboxia. *Global Biogeochemical Cycles*, *22*, GB4008. http://doi.org/10.1029/2007GB003147

Palter, J. B., & Trossman, D. S. (2018).The sensitivity of future ocean oxygento changes in ocean circulation. *GlobalBiogeochemical Cycles*, *32*, 738–751. https://doi.org/10.1002/2017GB005777

Qin Xuerong, Menviel Laurie, Sen Gupta Alex, & Sebille Erik (2016). Iron sources and pathways into the Pacific Equatorial Undercurrent. *Geophysical Research Letters*, *43*, 9843–9851. https://doi.org/10.1002/2016GL070501

Resplandy, L. (2018). Will ocean zones with low oxygen levels expand or shrink? *Nature*, *557*(7705), 314. Retrieved 2018-09-13TZ, from https://doi.org/10.1038/d41586-018-05034-y

Resplandy, L., Keeling, R. F., Rödenbeck, C., Stephens, B. B., Khatiwala, S., Rodgers, K. B., et al. (2018). Revision of global carbon fluxes based on a reassessment of oceanic and riverine carbon transport. *Nature Geoscience*, *11*, 504–509. Retrieved 2018-06-12TZ, from https://doi.org/10.1038/s41561-018-0151-3

Schmidtko, S., Stramma, L., & Visbeck, M. (2017). Decline in global oceanic oxygen content during the past five decades. *Nature*, *542*(7641), 335. Retrieved 2017-11-30TZ, from https://doi.org/10.1038/nature21399

Séférian, R., Gehlen, M., Bopp, L., Resplandy, L., Orr, J. C., Marti, O., et al. (2016). Inconsistent strategies to spin up models in CMIP5: Implications for ocean biogeochemical model performance assessment. *Geoscientific Model Development*, *9*(5), 1827–1851. Retrieved 2018-04- 24TZ, from https://www.geosci-model-dev.net/9/1827/2016/

Shigemitsu, M., Yamamoto, A., Oka, A., & Yamanaka, Y. (2017). One possible uncertainty in CMIP5 projections of low oxygen water volume in the Eastern Tropical Pacific. *Global Biogeochemical Cycles*, *31*, 804–820. https://doi.org/10.1002/2016GB005447

Sperling, E. A., Frieder, C. A., Raman, A. V., Girguis, P. R., Levin, L. A., & Knoll, A. H. (2013). Oxygen, ecology, and the Cambrian radiation of animals. *Proceedings of the National Academy of Sciences*, *110*(33), 13,446–13,451. Retrieved 2019-01-17TZ, from https://www.pnas.org/content/110/33/13446. https://doi.org/10.1073/pnas.1312778110

Stramma, L., Johnson, G. C., Firing, E., & Schmidtko, S. (2010). Eastern Pacific oxygen minimum zones: Supply paths and multidecadal changes. *Journal of Geophysical Research*, *115*, C09011. https://doi.org/10.1029/2009JC005976

Stramma, L., Johnson, G. C., Sprintall, J., & Mohrholz, V. (2008). Expanding oxygen-minimum zones in the tropical oceans. *Science*, *320*(5876), 655–658. Retrieved 2018-09-13TZ, from http://science.sciencemag.org/content/320/5876/655, https://doi.org/10.1126/science.1153847

Stramma, L., Prince, E. D., Schmidtko, S., Luo, J., Hoolihan, J. P., Visbeck, M., et al. (2012). Expansion of oxygen minimum zones may reduce available habitat for tropical pelagic fishes. *Nature Climate Change*, *2*(1), 33–37. Retrieved 2019-01-17TZ, from https://www.nature.com/articles/nclimate1304

Taylor, K. E., Stouffer, R. J., & Meehl, G. A. (2011). An Overview of CMIP5 and the experiment design. *Bulletin of the American Meteorological Society*, *93*(4), 485–498. Retrieved 2019-01-07TZ, from https://journals.ametsoc.org/doi/abs/10.1175/BAMS-D-11-00094.1

Yang, S., Gruber, N., Long, M. C., & Vogt, M. (2017). ENSO-driven variability of denitrification and suboxia in the Eastern Tropical Pacific Ocean. *Global Biogeochemical Cycles*, *31*, 1470–1487. https://doi.org/10.1002/2016GB005596

Erratum

In the originally published version of this article, there was an error in the legend of Figure 5. This error has since been corrected, and the present version may be considered the authoritative version of record.